Earth Planets Space, **56**, 259–268, 2004

Fog observations with a millimeter-wave scanning radar at Miyoshi basin, Japan

Michihiro Teshiba[1], Hiroyuki Hashiguchi[1], Akihisa Uematsu[1], Hisamichi Tanaka[2], Yasunobu Ohmori[2], and Shoichiro Fukao[1]

[1]*Radio Science Center for Space and Atmosphere, Kyoto University, Uji, Kyoto 611-0011, Japan*
[2]*Communication Systems Center, Mitsubishi Electric Corporation 8-1-1 Tsukaguchi-honmachi, Amagasaki 661-8661, Japan*

(Received September 8, 2003; Revised February 24, 2004; Accepted February 24, 2004)

A special fog observation campaign was conducted in the Miyoshi basin, Hiroshima prefecture, Japan during the period November 7–15, 2000. We observed the spatial distributions of fogs and their movements using a millimeter-wave scanning radar. This is the first time that the distribution of basin fogs associated with fog development and decay processes has been examined. Echo intensity observed with the radar, which is mainly associated with fog particle size, was almost under −23 dBZ at levels below 200 m in height. The horizontal distribution of echo intensity changed with time. Namely, weak echoes were observed over nearly all observation areas at first, and then the echoes gradually became stronger as the fogs developed, although the echoes were weaker at higher levels. After sunrise, the echoes decayed. During the developing periods, the occurrence ratio of the echo intensity between −38 and −23 dBZ increased from the lower height, while the ratio decreased from the higher levels during the decay periods. This feature in the developing period is consistent with the results of optical measurements but the feature in the decaying period is inconsistent. It is suggested that this inconsistency is due to the difference in sensitivity between the two measurement approaches.

Key words: Fog, remote sensing, millimeter-wave radar, mesoscale meteorology, boundary layer meteorology.

1. Introduction

The Miyoshi basin, located in the west-central part of the main island of Japan, is well-known places for its fogs which frequently appear in autumn. Fog observations using cameras have been conducted by the observation group of the Hiroshima Prefectural Women's University (Miyata, 1994). This group examined the surface structure of fogs associated with their development in Miyoshi basin. Fogs in various basins have been studied in other countries (e.g., Pilie *et al*., 1975a, b; Mason, 1982; Kunkel, 1984; Kidron *et al*., 2000; Kidron, 2000) as well as in Japan (e.g., Sawai, 1982; Shimohata, 1992; Research society of climate in a small area, 1994). All of these studies examined only the surface structure of fogs, because so far it has been difficult to observe the inner structure of fogs. For instance, the sodar can observe the wind profiles inside of fogs, but the observation area is limited to regions just above the sodar so that the horizontal structure cannot be obtained. A millimeter-wave (mm-wave) radar can observe the three-dimensional distributions of fog particles and their movement (Hamazu *et al*., 2003), which is not detectable with C-band (5.6 GHz frequency) meteorological radars (Sauvageot, 1992), such as the operational meteorological radars of the Japan Meteorological Agency (JMA). Mm-wave radars also have been used for cloud studies (e.g., Kropfli *et al*., 1984; Pasqualucci, 1984).

In contrast to fog observations in basins, many observations have been conducted concerning sea fogs at Kushiro, Hokkaido, Japan during the summer season (e.g., Uyeda and Yagi, 1984; Sea fogs research team, 1985; Yanagisawa *et al*., 1986; Yamamoto *et al*., 2001). Uyeda and Yagi (1984) studied sea fogs in an urban area and in the coastal suburbs, showing that sea fogs changed their characteristics at the coast, and that fogs over the urban area were denser than those over the coastal suburbs. Yanagisawa *et al*. (1986) studied sea fogs at Kushiro using a fixed-pointing mm-wave radar. They examined the relationship between the echo intensity and other meteorological parameters, such as the distribution of fog particles and the visibility at some observation sites. Our group has also observed sea fogs with mm-wave radars at Kushiro in the summer season of 1999–2002, and found the wave-like structure of fog echoes (Uematsu *et al*., 2004).

A mm-wave scanning Doppler radar (hereafter referred to as the mm-wave radar) has been employed in our fog studies. The radar, which was developed by our group, has a parabolic antenna of 2 m in diameter, 100 kW peak output power, and the radar frequency of 34.75 GHz (Hamazu *et al*., 2003). Moreover, the radar is mounted on a truck as shown in Fig. 1 for the convenience of observations at various places. It uses the double-pulse mode with 4500 and 450 pps (pulse per second) to obtain a maximum Doppler velocity of 9.7 m/s with the range resolution of 125 m. The azimuth resolution is 0.35°, which is associated with 12 m at 2 km range (Hamazu *et al*., 2003). We installed the mm-wave radar in the intensive observations of fogs conducted in Miyoshi basin, Hiroshima prefecture, Japan on November 7–15, 2000 (Tanaka *et al*., 2001a, b). Tanaka *et al*. (2001b) summarized observational results with cameras during this period. The period from 22 LT on November 13 to 10 LT on the next day was especially worth noting. While deep fogs were recorded by other observers, we found that the be-

Fig. 1. Outlook of the mm-wave radar.

Table 1. The number of echo intensity from −29 to −20 dBZ at the interval of 3 dBZ in the period from 23 to 9 LT every an hour in the observed area at 100 m height. During the period 7–8 LT, there are six datasets while there are eight in other periods, because of a system trouble of the radar around 7 LT.

Time	−29 ∼ −26 dBZ	−26 ∼ −23 dBZ	−23 ∼ −20 dBZ
23–0 LT	75	35	22
0–1 LT	76	26	25
1–2 LT	129	28	17
2–3 LT	325	33	19
3–4 LT	619	102	13
4–5 LT	767	104	22
5–6 LT	1031	128	19
6–7 LT	792	197	15
7–8 LT	251	27	11
8–9 LT	73	28	30

havior of fogs corresponded to the developing and decaying processes of fogs around the bottom of Miyoshi basin, which was investigated using echo intensity data observed with the mm-wave radar.

2. Methodology of the mm-wave Radar

We operated the mm-wave radar in CAPPI (Constant Altitude Plan Position Indicator) mode of seven elevation angles of 3.9°, 4.6°, 5.5°, 7.6°, 11.2°, 21.7°, and 90° with 1 rpm. The dataset was constructed at grid-points every seven minutes, whose grid size was 100 m horizontally and 50 m vertically with a linear interpolation.

Echo intensity is proportional to the third power of fog particle diameter when the liquid water content (LWC) is constant, while it is also proportional to LWC when the size distribution of fog particles is constant (Sauvageot, 1992; Hamazu *et al*., 2003). That is, echo intensity is concerned with both the number and diameter of fog particles. Therefore, we can consider that the change of echo intensity is associated with the development of fogs. The mm-wave radar can provide Doppler velocity as well as echo intensity. Doppler velocity data, however, fluctuates very much, because fog particles move considerably during the span of seven minutes, and there are few relationships between these datasets. Therefore, in this paper, we use only the data of echo intensity.

Hamazu *et al*. (2003) showed that the minimum detectable radar reflectivity factor of this radar was about −38 dBZ at the range of 2.5 km from the radar. So the data showing echo intensities of less than −38 dBZ may be noise. On the other hand, the data stronger than −23 dBZ are regarded as clutter echoes because there was no rain around the radar site in the observed period. In this study, the number of echoes with intensities above −23 dBZ in a horizontal place at a specific height did not change with time in the observed area, especially at lower heights. For example, the numbers of echoes around −23 dBZ every hour at 100 m height are shown in Table 1. The number between −23 and −20 dBZ changed little in time in contrast to that between −26 and −23. Therefore, we regard echoes stronger −23 dBZ as clutter echoes. Unfortunately, we cannot use the data nearer than 0.8 km from the radar due to the limitations of the mm-wave radar system.

Miyoshi basin consists of a large central basin and small basins around it (see Fig. 2). The bottom of the basin, in which the mm-wave radar was installed, is about 155 m above sea level. Except for the region surrounded by the dashed line in the bottom panel of Fig. 2, the area contains

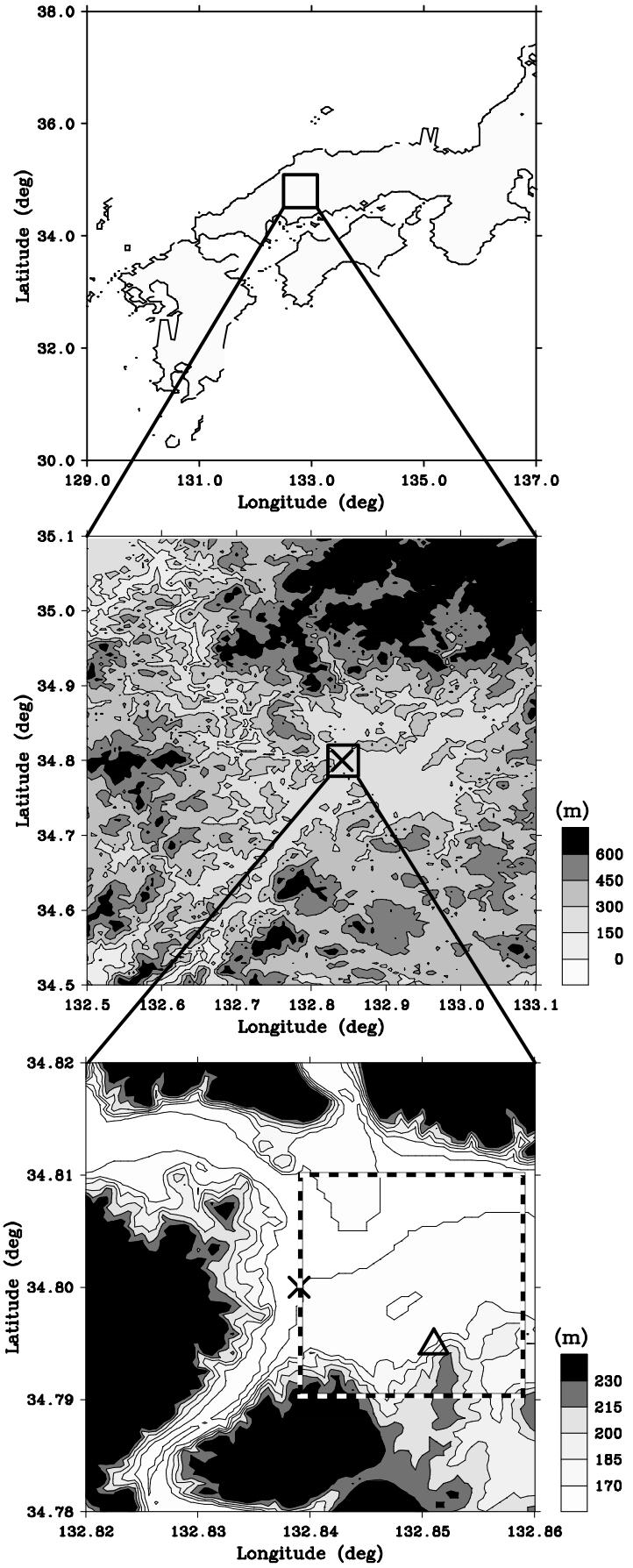

Fig. 2. Topography of Miyoshi basin. Cross symbols (×) indicate the position of the mm-wave radar. The dashed square in the bottom panel shows the area of the CAPPI plots in Figs. 6 and 7, and the area of the total data when calculating the occurrence frequency in Figs. 8 and 9. The surface meteorological instruments were installed at the position △. (Original topography data are 50 m grid of a global digital elevation model of the Geographical Survey Institute of Japan).

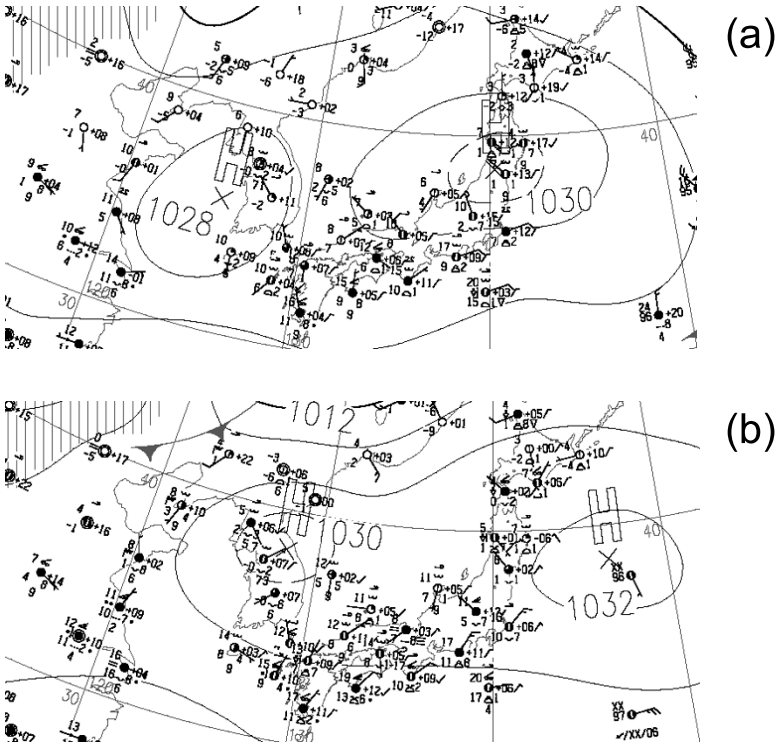

Fig. 3. Surface weather maps (a) at 12Z (21 LT) on November 13, 2000 and (b) at 00Z (09 LT) on November 14, 2000.

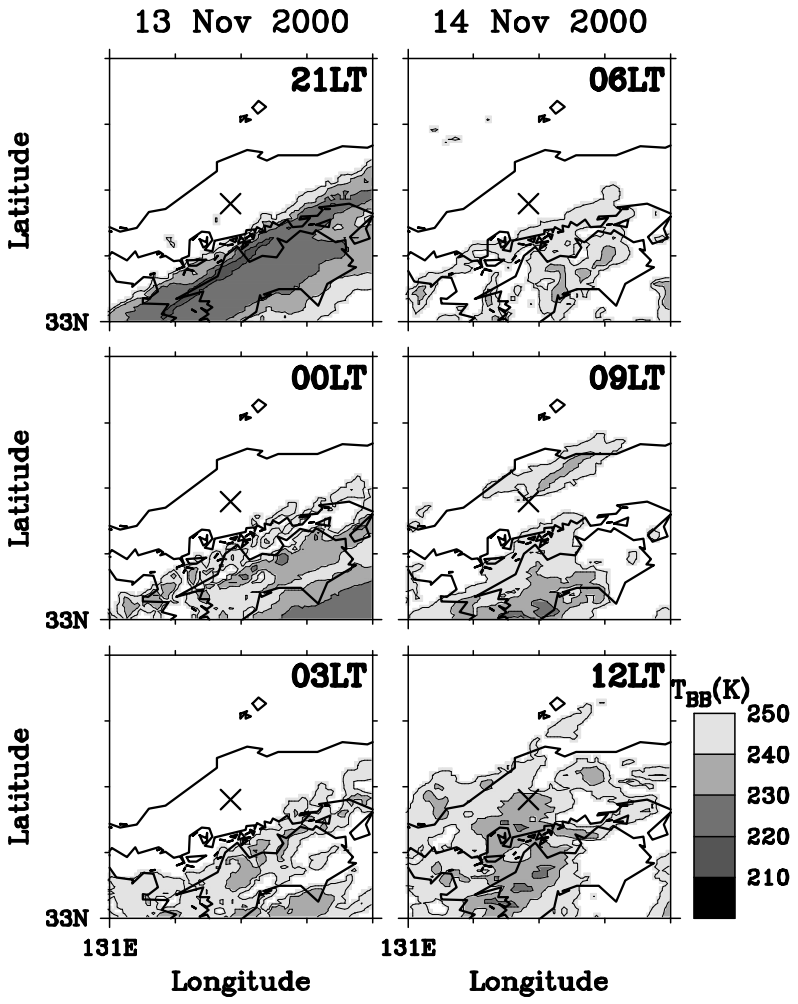

Fig. 4. IR imageries of the GMS every 3 hours from 21 LT on November 13 to 12 LT on the next day. Cross symbols (×) indicate the position of the mm-wave radar.

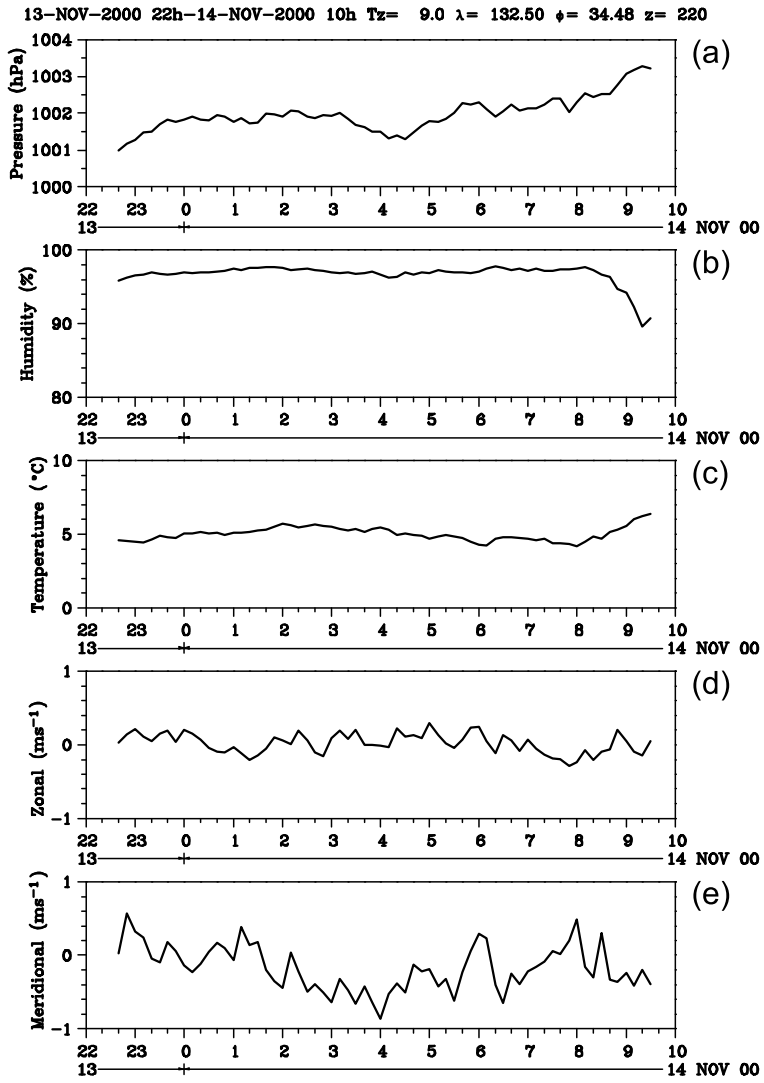

Fig. 5. Temporal variations of (a) pressure, (b) temperature, (c) relative humidity, (d) zonal wind component, and (e) meridional wind component on the ground at about 1.5 km southeast from the radar site at △ position in Fig. 1 every 10 minutes from 22 LT on November 13 to 10 LT on the next day.

mountains and hills and we cannot ignore the influence of clutter echoes. So we used the data between −38 and −23 dBZ of echo intensity[1] in the 2 km × 2 km area marked as a dashed square area in the figure, except for the range within 0.8 km from the radar.

3. Synoptic Situation

Figures 3(a) and (b) show surface weather maps at 12Z (21 LT) on November 13 and 00Z (09 LT) on November 14, respectively, provided from JMA. An area of high pressure moved eastward slowly, covering the Japan islands. Thin upper clouds seemed to cover the Miyoshi basin from the observation data at the Hamada meteorological station, located 70 km west of the basin, and also from the visible and infrared (IR) imageries of the Geostationary Meteorological Satellite (GMS) in Fig. 4 (only IR imageries are shown). So there are fully potentials of fogs' development around the Miyoshi basin. Figure 5 shows the surface data at about 1.5 km southeast from the radar site. In the observed period, there was no rain (not shown), the relative humidity was above 90% (it was nearly 96% before 8 LT), and the horizontal wind was very weak. After 8 LT, the relative humidity suddenly decreased in response to increasing temperature. This was considered to correspond to the sunrise and the weakness of the radiation cooling.

4. Distributions of Echo Intensity Data

Figures 6 and 7 show time series of horizontal distributions of radar echo intensity at 100 m height from the radar during 22–03 LT and 05–09 LT, respectively. As shown in Fig. 6, the echo intensity in the observed area gradually became stronger with time except for the south-east region where there exists a small hill. On the other hand, Figure 7 shows the echo intensity weakening by degrees with time. Therefore, we consider that the former and latter are associated with the development and the decay of fogs, respectively, because the change of the liquid water content (LWC) and/or the diameter of fog particles are associated with echo intensity as mentioned above. Hereafter, we call the periods

[1]If we assume LWC of 0.05 g/m^3 and monodisperse fog particles, echo intensity of −38 dBZ and −23 dBZ corresponds to fog particle diameters of about 10 and 30 μm in the diameter of fog particles, respectively (Hamazu *et al.*, 2003).

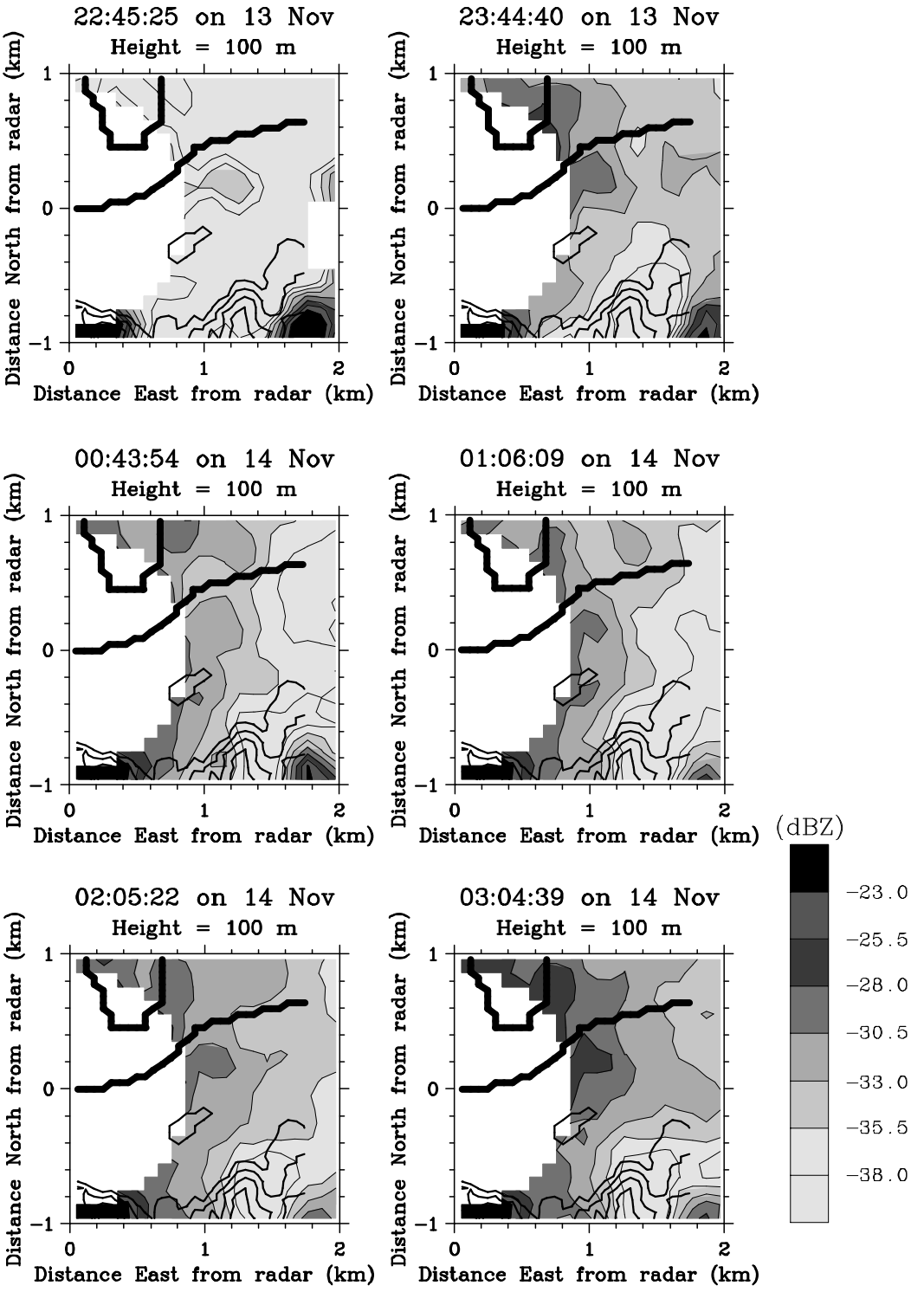

Fig. 6. Horizontal distributions of echo intensity observed from 2245 LT on November 13, 2000 to 0304 LT on the next day (in the developing period). Thick and thin curves indicate the border of the rivers and the topography every 12.5 m, respectively. The border of the rivers is about 155 m in altitude.

around 22–03 LT and 06–09 LT the developing and decaying periods, respectively. Strongest echo intensity is observed around 0.8 km distance from the radar. It means that the fog is developed most at the bottom of the basin, where the radar was located.

As mentioned above, echo data above −23 dBZ did not change in time at 100 and 200 m height, because the echo was caused by radar clutter, such as hills. Therefore, we calculated the number of data (grid points) from −38 to −23 dBZ at intervals of 2.5 dBZ at every 100 m height, which is defined as "the occurrence frequency". Figure 8 shows the occurrence frequency of fogs at heights of (a) 100 m, (b) 200 m, and (c) 300 m. The occurrence frequency between −38 and −30.5 dBZ at 100 m height increased before 0 LT. At the 100 and 200 m levels, the occurrence frequency between −30.5 and −25.5 dBZ increased during the period 1–4 LT

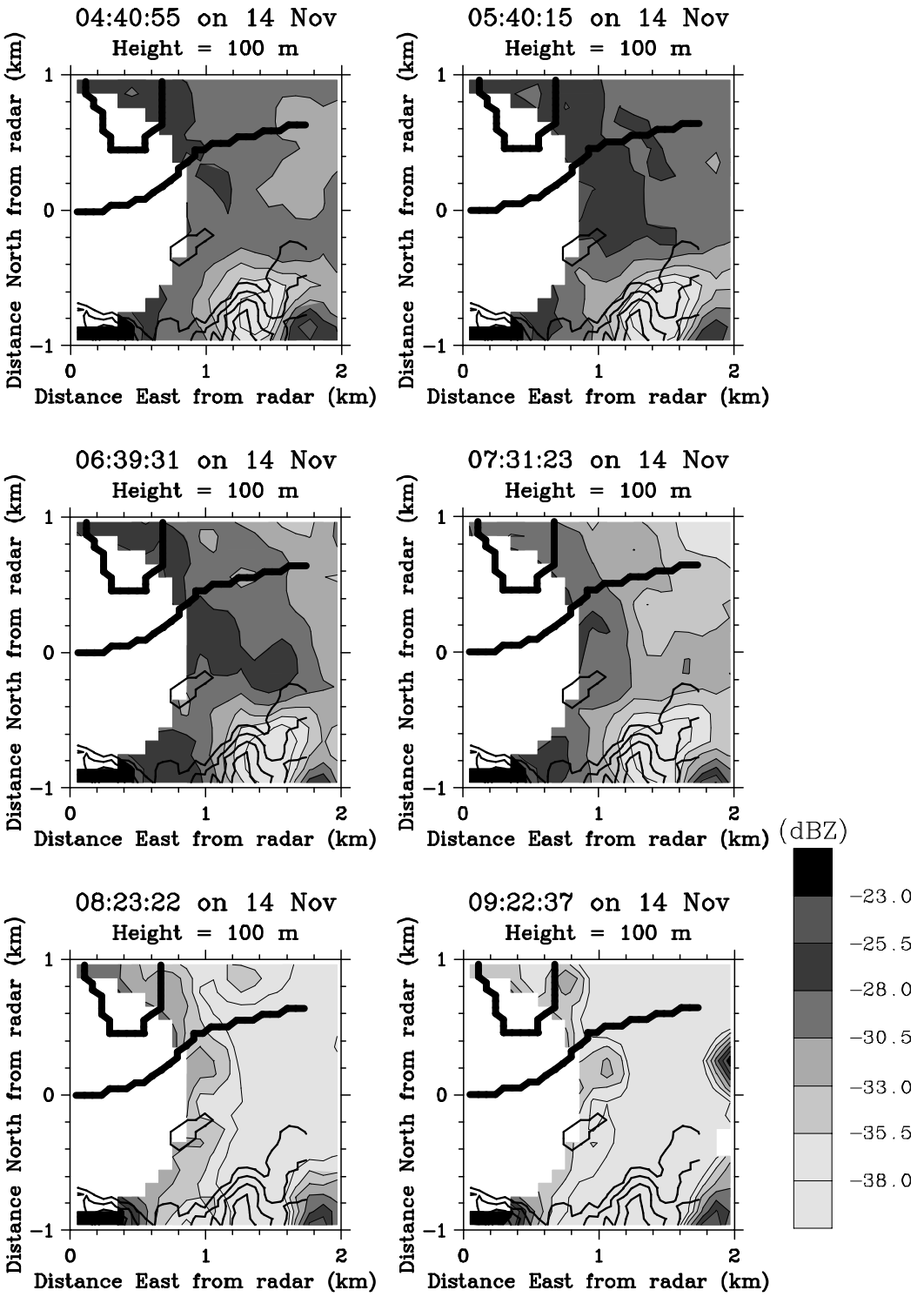

Fig. 7. Same as Fig. 6 but for 0440–0922 LT on November 14, 2000 (in the decaying period).

(the developing period) and decreased between 6–8 LT (the decaying period), while the total number did not so change. After fogs had developed, the occurrence frequency between −30.5 and −25.5 dBZ during 4–6 LT was dominant. The occurrence frequency at 300 m height below −30.5 dBZ was also dominant. The changes of the occurrence frequency at the 100 and 200 m levels during 1–4 and 6–8 LT were nearly the same, except that the number between −33 and −30.5 dBZ increased more at the 200 m level than at 100 m.

5. Developmental Behavior of Fogs

In this section, we ignore the difference in echo intensity between −38 and −23 dBZ. Although such a difference is also an indicator of fog development, we seek instead to investigate the spatial changes of fogs in terms of horizontal and vertical expansion, rather than the development of the density and diameter of fog particles. Figure 9 shows the occurrence ratio of fogs in the height range from 100 to 500 m height at 100 m intervals. The figure allows us to exam-

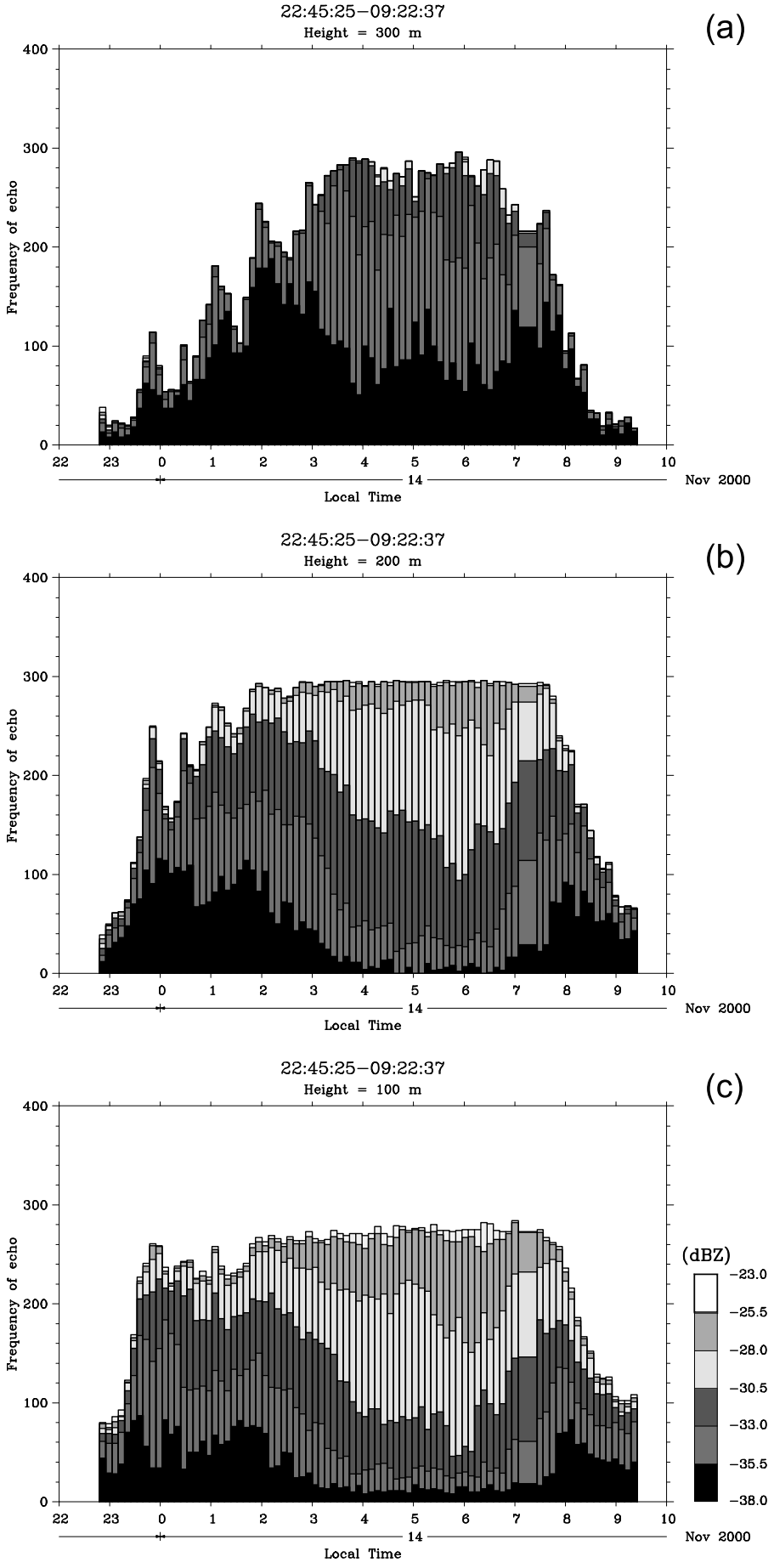

Fig. 8. Occurrence frequency of echo intensity from −38 to −23 dBZ at the interval of 6 dBZ at the heights of (a) 100 m, (b) 200 m, and (c) 300 m.

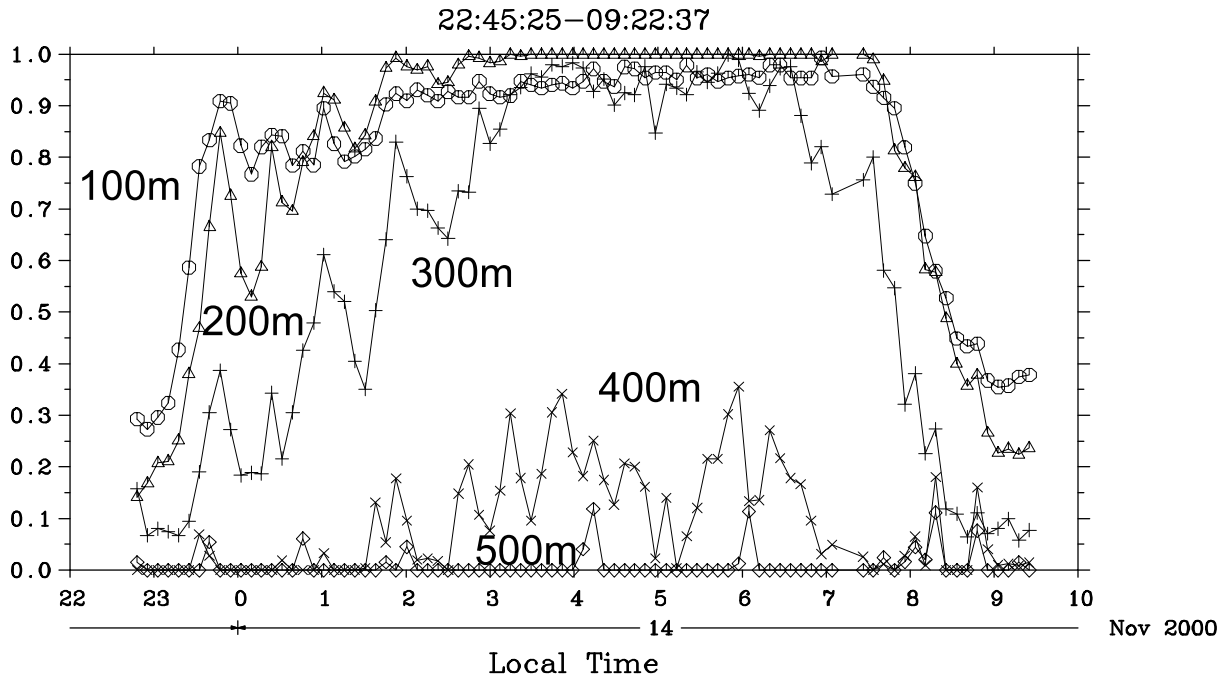

Fig. 9. Occurrence ratio of echo intensity from −38 to −23 dBZ at the interval of 100 m height. ◯, △, +, ×, and ◇ indicate data in the height range from 100 to 500 m at 100 m intervals, respectively.

ine the time variations of fogs with height, as well as aspects of the development and decay of fogs. The occurrence ratio is defined as the ratio of the number of data between −38 and −23 dBZ to the total number of 100-m grid data at each height in the observed area; the latter is the dashed square area in the bottom panel of Fig. 2, except for the range within 0.8 km of the radar. The increase of the occurrence ratio at both 100 and 200 m heights was remarkable during the hours 23–0 LT, which was the beginning of the developing period. After that, the occurrence ratio gradually increased. At 300 m, the occurrence ratio was gradually increasing during 23–4 LT. At 100 and 200 m heights, the occurrence ratio exceeded 0.8 during 1–8 LT. So we can consider that fogs covered nearly all the area at 100 and 200 m heights until 0 LT in the beginning of the fog development, and then expanded gradually to the surroundings areas. At a height of 300 m, the occurrence ratio increased and decreased during the developing and decaying period, respectively. It exceeded 0.9 during 3–6 LT, when fogs below 300 m were well developed. On the other hand, at 400 m, the occurrence ratio was small and fogs were not distributed horizontally. At the 500 m level, the ratio was very small. The top height of fogs observed with the mm-wave radar was between 300 and 500 m, because the occurrence ratio of fogs at a height of 500 m was much smaller than that at 300 or 400 m.

In general, we observed that the occurrence ratio gradually increased from lower height, that is, the increase started at nearly the same time at 100 and 200 m, and then it began at 300 m a few hours later. On the other hand, the ratio decreased first at higher levels, that is, the decrease started at 300 m, and then later at 100 and 200 m, where the ratio decreased simultaneously. We found that fogs developed from lower height and decay from higher height, as shown in Fig. 9.

6. Concluding Remarks

Generally speaking, the development of fogs is associated with an increase in the density and/or the diameter of fog particles, and also an increase in echo intensity. We examined fog behavior using echo intensity data obtained with the mm-wave radar during the intensive observation campaign conducted in the Miyoshi basin, Hiroshima, Japan during the period November 7–15, 2000.

We first investigated the time variations in horizontal fog distribution, and obtained strong echoes associated with the development of fogs. The strongest echo intensity around 0.8 km distance from the radar indicated that the fog developed especially at the bottom of the basin. Next, we looked at the occurrence frequency of echo intensity at each height. Below a height of 200 m, the occurrence frequency between −32 and −23 dBZ was dominant when fogs developed sufficiently. The change of the occurrence frequency at the 100 m level was similar to that at 200 m. The relatively strong echo was observed at the lower height, because the fog develops at the lower height. Finally, we examined the occurrence ratio of fog echoes at each height.

From the time variations of the occurrence ratio, we found that fogs developed from the surface and then decayed from their upper layer. In summary, these features observed with the mm-wave radar are consistent with camera observations in the developing stage, but differ from those previous observations during the decaying stage. This is because the mm-wave radar is more sensitive to fog droplet size, while cameras are mainly sensitive to droplet number density.

In this paper, we have demonstrated the potential of the mm-wave radar for fog studies. The differences at each height mean that the distributions of fog particles at each level are different each other, such a difference has not been observed by any other observations. In this observation, be-

cause the time resolution is not sufficient for a fog observation, the movement of fog particles cannot be directly observed. Moreover, simultaneous observations with the radar and other instruments are needed, because only the radar observation cannot divide the information of the echo intensity into that of the diameter and the density of fog particles. In future works, more observation campaigns, using the mm-wave radar and other instruments simultaneously, are required to examine the distribution and the movement of fog particles, and the difference in the decaying period.

Acknowledgments. The observation campaign was conducted by the Miyoshi Fog Observation Group including Dr. Masaaki Tanaka and Prof. Kenji Miyata. We thank Dr. Gernot Hassenpflug for his careful reading of the original manuscript. The present study was financially supported by Grants-in-Aids (12740270) of the Japan Society for the Promotion of Science (JSPS).

References

Hamazu, K., H. Hashiguchi, T. Wakayama, T. Matsuda, R. J. Doviak, and S. Fukao, A 35-GHz scanning Doppler radar for fog observations, *J. Atmos. Ocean. Tech.*, **20**, 972–986, 2003.

Kidron, G. J., Analysis of dew precipitation in three habitats within a small arid drainage basin, Negev Highlands, Israel, *Atmos. Res.*, **55**, 257–270, 2000.

Kidron, G. J., A. Yair, and A. Danin, Dew variability within a small arid drainage basin in the Negev Highlands, Israel, *Quart. J. Royal. Meteorol. Soc.*, **126**, 63–80, 2000.

Kropfli, R. A., W. R. Moninger, and F. Pasqualucci, Circular depolarization ratio and Doppler velocity measurements with a 35-GHz radar during the Cooperative Convective Precipitation Experiment, *Radio Science,* **19**, 141–147, 1984.

Kunkel, A. B., Parameterization of droplet terminal velocity and extinction coefficient in fog models, *J. Clim. Appl. Meteor.*, **23**, 34–41, 1984.

Mason, S. J., The physics of radiation fog, *J. Meteor. Soc. Japan,* **60**, 486–499, 1982.

Miyata, K., *Study of Fogs in the Miyoshi Basin,* 255 pp, Keisuisha Co., Ltd., 1994 (in Japanese).

Pasqualucci, F., Drop size distribution measurements in convective storms with a vertically pointing 35-GHz Doppler radar, *Radio Science,* **19**, 177–183, 1984.

Pilie, J. R., E. J. Mack, W. C. Kocmond, C. W. Rogers, and W. J. Eadie, The life cycle of valley fog. Part I: Micrometeorological characteristics, *J. Appl. Meteor.*, **14**, 347–363, 1975a.

Pilie, J. R., E. J. Mack, W. C. Kocmond, C. W. Rogers, and W. J. Eadie, The life cycle of valley fog. Part II: Fog Microphysics, *J. Appl. Meteor.*, **14**, 364–374, 1975b.

Research society of climate in a small area, On characteristic features of the basin fog at Ena district, *Tenki,* **No. 41-1**, 23–35, 1994 (in Japanese).

Sauvageot, H., *Radar Meteorology*, Artech House, Inc., Boston, 92, 1992.

Sawai, T., Understanding fog structure, *Tenki,* **29**, 731–747, 1982 (in Japanese).

Sea fogs research team, Observations of sea fog in Kushiro district, *Tenki,* **32**, 41–52, 1985 (in Japanese).

Shimohata, I., On the morning fog observed in Hida, *Tenki,* **No. 39-9**, 27–29, 1992 (in Japanese).

Tanaka, M., K. Miyata, T. Maitani, T. Hayashi, Y. Itoh, M. Horiguchi, T. Terao, T. Iwata, and Y. Ohashi, Intensive Fog Observations over Miyoshi Basin, *Annuals of Disaster Prevention Research Institute, Kyoto University,* **No. 43 B-1**, 185–209, 2000 (in Japanese).

Tanaka, M., K. Miyata, T. Maitani, T. Hayashi, Y. Ito, M. Horiguchi, T. Terao, T. Iwata, Y. Ohashi, K. Miyashita, M. Ohara, and H. Hashiguchi, Studies on the local circulations and fog formations over the basin, *Disaster Prevention Research Institute, Kyoto University,* **12G-16**, 3–77, 2001a (in Japanese).

Tanaka, M., K. Miyata, T. Maitani, T. Hayashi, Y. Itoh, M. Horiguchi, T. Terao, T. Iwata, Y. Ohashi, M. Oohara, K. Miyashita, H. Hashiguchi, and M. Teshiba, Intensive Fog Observations over Miyoshi Basin (Part II), *Annuals of Disaster Prevention Research Institute, Kyoto University,* **No.44 B-1**, 37–69, 2001b (in Japanese).

Uematsu, A., H. Hashiguchi, M. Teshiba, H. Tanaka, K. Hirashima, and S. Fukao, Moving cellular structure of fog echoes obtained with a millimeter-wave scanning Doppler radar at Kushiro, Japan, *J. Appl. Meteorol.*, 2004 (submitted).

Uyeda, H. and T. Yagi, Observation of sea fogs at the urban area and the coastal suburbs in Kushiro city, Hokkaido, *Tenki,* **31**, 137–145, 1984 (in Japanese).

Yamamoto, A., K. Akaeda, and O. Suzuki, The evaluation of the airport fog observation radar, *Abst. of 2nd Intern. Conf. on Fog and Fog Collection,* **2**, 391–394, 2001.

Yanagisawa, Z., M. Ishihara, and T. Sawai, Observations of sea fogs by 8.6 millimeter radar, *Tenki,* **33**, 603–612, 1986 (in Japanese).

M. Teshiba (e-mail: teshiba@kurasc.kyoto-u.ac.jp)